High-Precision Ramsey-Comb Spectroscopy at Deep Ultraviolet Wavelengths

R. K. Altmann, S. Galtier, L. S. Dreissen, and K. S. E. Eikema

LaserLaB, Department of Physics and Astronomy, VU University Amsterdam,
De Boelelaan 1081, 1081 HV Amsterdam, Netherlands

(Received 28 June 2016; published 20 October 2016)

High-precision spectroscopy in systems such as molecular hydrogen and helium ions is very interesting in view of tests of quantum electrodynamics and the proton radius puzzle. However, the required deep ultraviolet and shorter wavelengths pose serious experimental challenges. Here we show Ramsey-comb spectroscopy in the deep ultraviolet for the first time, thereby demonstrating its enabling capabilities for precision spectroscopy at short wavelengths. We excite ^{84}Kr in an atomic beam on the two-photon $4p^6 \rightarrow 4p^5 5p[1/2]_0$ transition at 212.55 nm. It is shown that the ac-Stark shift is effectively eliminated, and combined with a counterpropagating excitation geometry to suppress Doppler effects, a transition frequency of 2 820 833 101 679(103) kHz is found. The uncertainty of our measurement is 34 times smaller than the best previous measurement, and only limited by the 27 ns lifetime of the excited state.

Precision laser spectroscopy has made great advances since the invention of the frequency-comb laser [1,2] because these devices enable optical frequencies to be counted and compared to atomic frequency standards. This has resulted in impressively accurate tests of bound-state quantum electrodynamics (QED), e.g., based on precision spectroscopy of atomic hydrogen [3–5]. However, in 2010 spectroscopy of muonic hydrogen has led to a discrepancy with theory that is now known as the proton radius puzzle [6,7]. One approach to solve this puzzle is based on measuring more transition frequencies in muonic and electronic hydrogen. In particular, more measurements in electronic hydrogen are helpful to obtain an improved Rydberg constant (see, e.g., Refs. [8–10]), to disentangle the influence of this constant and the finite proton size effect. Also, spectroscopy of muonic helium ions is pursued [11] to test the finite-size effect of a different nucleus. In view of these efforts, two more systems are particularly interesting: $1S - 2S$ spectroscopy in electronic helium ions [11,12] and spectroscopy of *molecular* hydrogen [13,14]. Molecular hydrogen has also been used recently for searches of physics beyond the standard model, such as possible fifth forces [15]. In both systems the challenge is the short wavelengths required for electronic excitation from the ground state: deep UV for H_2 and extreme UV (XUV) for He^+, where no direct frequency combs are available.

To overcome this challenge, nonlinear optics with frequency-comb lasers is pursued to directly excite transitions with an up-converted comb laser [16,17]. The typical pulse energy of a few nJ of most comb lasers is not sufficient for that. One approach to increase the energy is based on full-repetition rate amplifiers and enhancement resonators to reach the required μJ-level pulse energy for intracavity high-harmonic generation [17–19]. Alternatively, one can amplify only two pulses from a

frequency-comb laser for high-harmonic generation [16]. This can lead to more efficient wavelength conversion and to higher two-photon transition probabilities. If then pulse pairs at multiple delays can be selected, precision spectroscopy via the Ramsey-comb method becomes possible [20] with orders of magnitude higher pulse energy (mJ/pulse in the IR and tens of μJ/pulse in the UV) than achievable with full repetition rate based methods. Previously we demonstrated these properties for near-infrared two-photon transitions of rubidium in a gas cell, showing that even with only two pulses, the accuracy and resolution of frequency combs can be recovered [20,21].

In this Letter we demonstrate that Ramsey-comb spectroscopy can be extended to much shorter wavelengths in the deep UV for the first time. This is illustrated by a 34-times improved frequency measurement in an atomic beam on the $4p^6 \rightarrow 4p^5 5p[1/2]_0$ two-photon transition in ^{84}Kr at $\lambda_c \approx 212.55$ nm.

Ramsey-comb spectroscopy is based on a series of measurements using only two phase-coherent pulses from a frequency-comb laser. Frequency-comb lasers are ideally suited for this purpose as they produce an infinite train of pulses with a well-defined repetition time (T_{rep}) and phase relation ($\Delta\phi_{\text{CEO}}$) between subsequent pulses. In the following description we assume excitation of a two-level atom with a transition frequency f_{tr}. Excitation with two selected comb laser pulses resembles Ramsey's method of separated oscillatory fields, which is the basis of most atomic clocks in the radio frequency and optical domain [22,23]. Each excitation pulse induces a superposition of the ground and excited state. Quantum interference between the two excitation contributions then leads to an excited state population (ρ_{22}), which depends on the exact time delay (Δt) and optical phase shift ($\Delta\phi$, including $\Delta\phi_{\text{CEO}}$) between the two excitation pulses:

$$\rho_{22}(\Delta t) \sim \cos(2\pi f_{\mathrm{tr}}\Delta t + \Delta\phi). \qquad (1)$$

By probing the excited state population as a function of Δt, traditional Ramsey fringes are observed from which the transition frequency can be determined. One issue with Ramsey spectroscopy is a possible spurious phase shift in the excitation pulses that is not accounted for [16,24]. With frequency-comb lasers this issue can now be solved in an elegant way if pulse pairs are selected at *different* multiples of the repetition time of the frequency-comb laser. One can then record signals at a series of delays equal to

$$\Delta t = \Delta N T_{\mathrm{rep}} + \delta t, \qquad (2)$$

where ΔN is an integer. To record a Ramsey signal at each ΔN, the repetition time of the laser is scanned by a small amount, δt. Combined with the larger time steps by changing ΔN this results in a series of recordings that together forms the "Ramsey-comb" signal [20]. The advantage of comparing signals from multiple pulse pairs is that any constant phase shift as a function of ΔN can be identified as a common influence. Therefore, it can be eliminated from the transition frequency determination even if the absolute value is unknown, which greatly enhances the accuracy. If the pulse energy is kept constant as a function of ΔN, the ac-Stark shift from the excitation pulses also manifests itself as a constant phase shift of the Ramsey signals, which can therefore be eliminated as well. Moreover, similar to traditional Ramsey spectroscopy, the accuracy of Ramsey-comb spectroscopy becomes better for longer time delays.

Experimentally, we create high-intensity pulse pairs by parametric amplification of pulses from a Kerr-lens mode-locked Ti:sapphire frequency-comb laser (see Fig. 1). The repetition frequency ($f_{\mathrm{rep}} = 126$ MHz) and carrier-envelope offset frequency ($f_{\mathrm{CEO}} = \Delta\phi_{\mathrm{CEO}}f_{\mathrm{rep}}/2\pi$) of the

comb laser are both referenced to a cesium atomic clock for absolute frequency and time calibration.

In a stretcher the pulses from the comb laser are spectrally clipped to 3 nm around 850.2 nm and chirped by 1.2×10^6 fs^2 of second-order dispersion to produce 12 ps pulses. These pulses seed a noncollinear optical parametric chirped-pulse amplifier (NOPCPA) where selectively two frequency-comb pulses are amplified up to 1.7 mJ. Strong saturation lengthens the amplified pulses further to more than 20 ps, and gives the pulse a double-peak structure in spectrum and time evolution (see Fig. 1). The two 75 ps pump pulses at 532 nm wavelength for the NOPCPA are produced with a separate, synchronized laser system (see Refs. [25,26]).

The amplified frequency-comb pulses are frequency up-converted using three β-barium-borate (BBO) crystals, producing up to 45 μJ/pulse at 212.55 nm. The resulting deep UV beam is split in equal parts by a metallic beam splitter. This enables us to excite the two-photon transition in a counterpropagating laser beam configuration so that the first-order Doppler shift is reduced. The collision point of the excitation pulses is overlapped with an atomic beam based on a pulsed supersonic expansion of krypton atoms. The direction and divergence of the atomic beam is determined by a skimmer (circular opening 0.5 mm) and a subsequent slit of 3 mm width. After the excitation pulses, an ionization pulse at 532 nm is applied, which only ionizes krypton atoms that are in the excited state. The resulting ions are extracted with a pulsed electric field to enable field-free excitation. A time-of-flight drift tube is then used in combination with a channel-electron multiplier (CEM) to separate and detect the different isotopes with a mass resolution of $m/\Delta m = 212$ (FWHM). Each isotope is measured individually with a boxcar integrator (Stanford Research), and the whole experiment is repeated at a rate of 28.2 Hz.
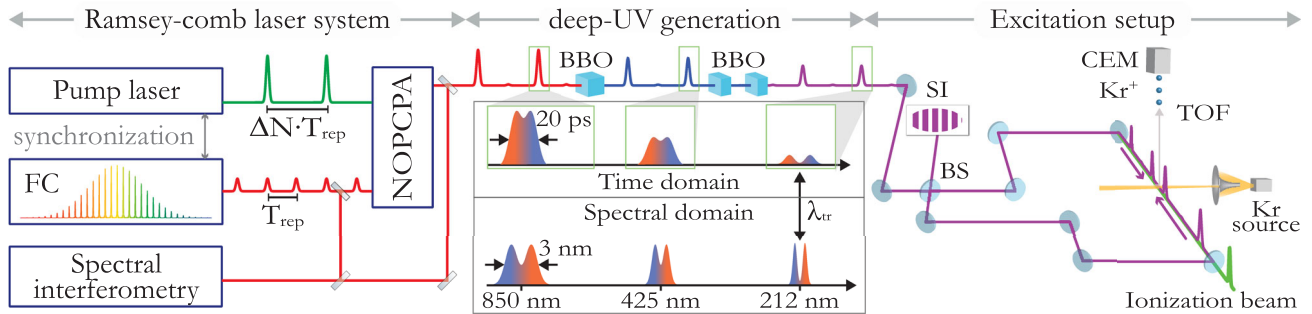

FIG. 1. Schematic overview of the setup. Frequency-comb (FC) pulse pairs are amplified in a noncollinear optical parametric chirped-pulse amplifier (NOPCPA). Spectral interferometry is used to measure the differential phase between the amplified and original frequency-comb pulses. The amplified pulse pairs are up-converted sequentially using three BBO crystals, and the two insets show the spectral and temporal evolution of each Ramsey comb pulse, starting with the original near-infrared spectrum and ending with a "red-blue" split pulse in the deep UV near $\lambda_{\mathrm{tr}} = 212.55$ nm. The UV beams are aligned exactly counterpropagating, using the fringes observed at the output of the metallic 50% beam splitter (BS), which acts as a Sagnac interferometer (SI). After excitation, the krypton atoms are ionized and extracted upwards in a time-of-flight (TOF) drift tube and detected with a channel-electron multiplier (CEM, EDR model from Dr. Sjuts Optotechnik GmbH).

With two counterpropagating ultrafast laser pulses, the two-photon transition can still be excited from just one side, leading to calibration errors and reduced signal contrast. This signal can be suppressed by strongly chirped pulses [27,28], or more effectively, by circularly polarized light, or a combination of both [20]. However, purely circularly polarized light is difficult to achieve for deep UV ultrafast laser pulses. Therefore, we use an alternative approach with linear polarized light pulses that are split in two parts, a "red" and a "blue" part relative to the transition frequency [29]. Combined with chirp in the pulses, their time evolution is also split into a red and a blue part. With this temporal and spectral shape the transition can only be excited when the red and blue parts of the pulses overlap from opposite sides, thereby fully suppressing excitation by a single side.

Experimentally this is realized by nonlinear up-conversion of the chirped fundamental pulses with three different frequency-doubling crystals (see Fig. 1). In the first BBO crystal (1.0 mm thick) the full bandwidth of the fundamental pulse is frequency doubled to ~425 nm. The second doubling stage, to the deep UV, is split up over two separate crystals. The thickness of these crystals (0.5 mm) is chosen such that the phase-matching condition is limited to a narrow spectral range (< 0.5 nm). Each crystal is only phase matched at one edge of the spectrum so that a double-peak structure is created in the deep UV with zero intensity at the two-photon resonance. Because of the large chirp introduced by the stretching, the temporal shape of the laser pulses will have a similar double-peak structure with the blue edge of the spectrum trailing the red edge (see in Fig. 1). The spatial separation of the two colors (~6.5 mm, equivalent to 20 ps) is larger than the width of the atomic beam (~3 mm), so we are able to observe the two collision points separately (where blue meets red and vice versa).

Using this setup Ramsey-comb signals for the ^{84}Kr isotope have been recorded up to 8 times the laser repetition time of 7.9 ns. Only a single transition is resonant within the bandwidth of the laser pulses; therefore, measuring Ramsey signals at two different ΔN suffices to eliminate common phase-shift effects and determine the transition frequency. We start at $\Delta N = 2$ to avoid transient effects, while the longest delay is typically chosen at $\Delta N = 7$ for optimal signal-to-noise ratio given the upper-state lifetime of ~27 ns. At each ΔN the repetition time of the laser is scanned over several hundreds of attoseconds to observe roughly two oscillation periods of the Ramsey signal (see Fig. 2). The fitting and frequency determination from a Ramsey-comb measurement is done purely on the phase of the recorded time-domain signals, as explained in Ref. [20,21]. The statistical uncertainty of a frequency measurement from the fit is based on the uncertainty of the individual measurement points, which in turn is determined by the signal fluctuations over approximately 350 laser shots.
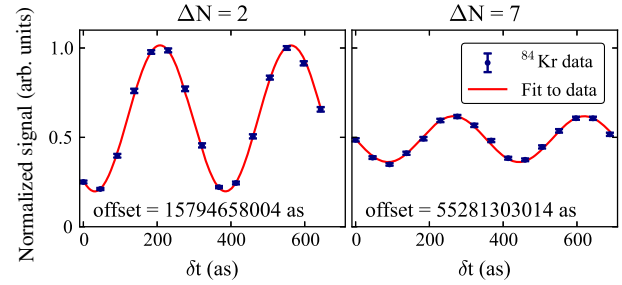

FIG. 2.   Example of measured Ramsey signals at $\Delta N = 2$ and $\Delta N = 7$. At each ΔN the delay time is scanned over ~700 attoseconds (as) and is offset by $\Delta N T_{\rm rep}$ [see Eq. (2)] corresponding to 15.79 and 55.28 ns, respectively, as indicated in the figure. Each data point is an average over 350 laser shots and the variation within this set is used to determine the statistical uncertainty of the data points. The signal is normalized to the maximum signal of the first Ramsey fringe. The red line is a fit to the data based on Eq. (1).

A misalignment of the laser beams with respect to the atomic beam or a residual angle between the counterpropagating laser beams both lead to a residual Doppler shift. Therefore, we align the deep UV beams as parallel as possible by monitoring the light transmitted through the beam splitter. This configuration forms a Sagnac interferometer, and with perfect alignment complete extinction is observed at the output [30]. A residual first-order Doppler shift can then still be present due to chirp of the excitation pulses, depending on the trajectory of the atoms through the laser beams [10]. However, this effect and other Doppler effects are minimized with a procedure based on measuring the transition frequency for different velocities of the atomic beam while adjusting the angle between the laser beams and the atomic beam until no more Doppler shift is observed. For this procedure the speed of the atomic beam was increased by mixing pure krypton [380(30) m/s] with at least 5 times more neon or helium, leading to a Kr velocity of 686(60) and 931(134) m/s, respectively. By extrapolating the measured transition frequencies to zero velocity, the Doppler-free transition frequency has been determined with a statistical uncertainty of 58 kHz (see Fig. 3). For each velocity class, the second-order Doppler shift was also taken into account (2.3 kHz for 380 m/s, 7.4 kHz for 686 m/s, and 13.6 kHz for 931 m/s). Furthermore, the measurements were performed in both deep UV collision points, giving consistent results.

Another potential source of systematic error is a phase-shift difference between the amplified frequency-comb pulses that depends on ΔN; it would lead to a frequency shift

$$\Delta f = \frac{8 \Delta \phi}{2\pi \Delta N T_{\rm rep}}, \tag{3}$$

where $\Delta \phi$ is the phase change between the two excitation pulse pairs (with a factor 8 for using the fourth harmonic on
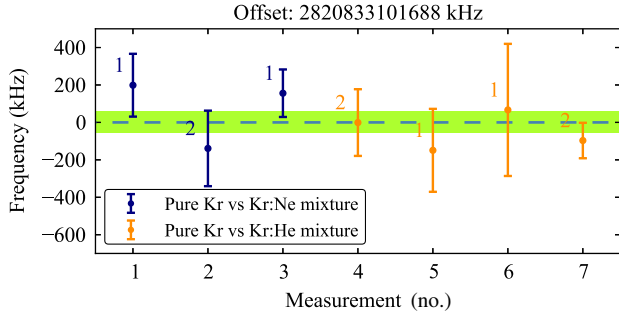
FIG. 3. Measurement results of the $4p^6 \rightarrow 4p^5 5p[1/2]_0$ transition frequency in ^{84}Kr. Each data point is an average over 10–20 Ramsey measurements at macrodelays $\Delta N = 2$ and $\Delta N = 7$, and the green band shows the 1σ uncertainty of the average. The first-order Doppler shift is determined by measuring the transition frequency difference for pure Kr with respect to Kr:Ne and Kr:He mixtures. The color indicates which noble gas was used to speed up the supersonic expansion, and the numeral indicates which collision point was used.

a two-photon transition). The laser system was designed to keep $\Delta\phi$ of the amplified pulses as constant as possible as a function of ΔN [26]. This is verified by measuring the phase difference between the amplified pulses and the original frequency-comb pulses with spectral interferometry [20]. Measurement results of the differential phase shift between $\Delta N = 2$ and $\Delta N = 7$ are shown in Fig. 4(a). This shows the combined phases from the red and blue part of the spectrum contributing to the two-photon transition. There is no significant phase change within the uncertainty
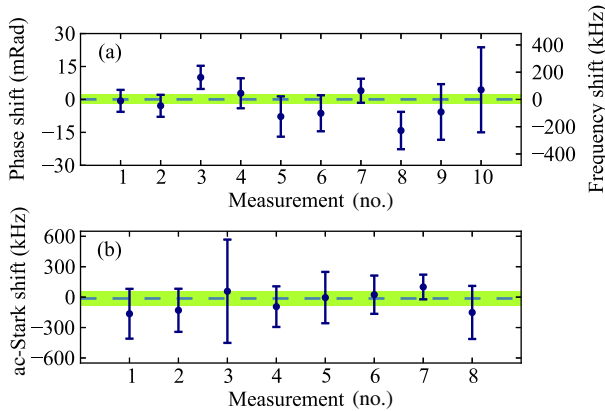

FIG. 4. (a) Results of the differential phase measurement on the fundamental pulses at 850 nm between the $\Delta N = 2$ and $\Delta N = 7$ pulse pairs. The blue and red part of the amplified pulse spectrum are measured separately from which the mean shift is calculated and shown in the graph. No significant phase shift is observed within an uncertainty of 2.1 mrad (indicated with the green band), corresponding to 35 kHz on the transition frequency. (b) Results of the ac-Stark shift determination. Each data point represents an average of 10–20 measurements. Within the uncertainty of 72 kHz (indicated by the green band), no shift due to the excitation light field is observed.

of 2.1 mrad (corresponding to 35 kHz uncertainty for the transition frequency).

The dc-Stark effect is tested by a comparison of measurements in a static 29.4 V/cm electric field, and in a zero electric field (< 0.17 V/cm), confirming a negligible ($\ll 1$ kHz) shift in the measured transition frequency.

The ac-Stark shift is suppressed by a factor of 100 by keeping the energy of the pulses constant to 1%. To detect any residual effect, we vary the pulse energy deliberately with a factor of 2 and extrapolate the measured transition-frequency difference to zero intensity. The determined residual ac-Stark shift of $-13(72)$ kHz [see Fig. 4(b)] is consistent with zero. Because the pulse energy was varied by reducing the infrared intensity, this simultaneously excludes effects induced in the frequency up-conversion stages.

The separation of different isotopes in a TOF can be a potential source of systematic error. Isotopes that arrive early on the detector can modify the detector gain experienced by the isotopes that arrive later [31]. However, the natural abundance of ^{82}Kr and ^{83}Kr compared to ^{84}Kr is 5 times less and is therefore expected to have minimal influence. Any residual effect can be experimentally detected as a variation of the measured ^{84}Kr Ramsey signal phase when ΔN is changed, caused by the different Ramsey-signal phases of the other isotopes for each ΔN. No effect was detected when varying ΔN for all values between 2 and 8, with a resulting uncertainty margin of 25 kHz for the transition frequency.

Finally, we tested for a Zeeman shift by applying a magnetic field 8 times higher than Earth's magnetic field. As expected for the $m_j = 0$ states, no shift was detected, excluding effects with an uncertainty of 13 kHz for the transition.

Taking all measurements into account (see Table I), we arrive at a frequency of 2 820 833 101 679 kHz with a 1σ uncertainty of 103 kHz (a relative uncertainty of

TABLE I. Contributions to the $4p^6 \rightarrow 4p^5 5p[1/2]_0$ transition frequency in ^{84}Kr with their respective uncertainties. All values are listed in kHz.

Contribution	Experimental value	1σ
Transition frequency[a]	2 820 833 101 688	58
ac-Stark shift	−13	72
dc-Stark effect	0	0
Laser phase shift	1	35
Gain depletion[b]	0	25
Zeeman shift	3	13
Total	2 820 833 101 679	103

[a]Corrected for the first and second Doppler shift (see text). The quoted uncertainty here is statistical.
[b]A shift due to detector saturation combined with different arrival times of the isotopes.

3.7×10^{-11}) for the $4p^6 \rightarrow 4p^5 5p[1/2]_0$ transition in ^{84}Kr. This result is 34 times more accurate and in agreement with the most accurate previous measurement [24], demonstrating the power of the Ramsey-comb method for transitions in the deep UV wavelength range. The accuracy is mainly limited by the short lifetime (27 ns) of the excited state, because that determines the maximum pulse delay. This is particularly promising for spectroscopy on the $EF \leftarrow X$ transition in molecular hydrogen, as the excited state (for vibrational quantum number $\nu = 0$) has a lifetime of 200 ns. Potentially, a frequency accuracy significantly better than 50 kHz might therefore be reached. That would be 2 orders of magnitude better than previous experiments [32], providing new opportunities to test QED and the proton size with H_2 molecules. Similarly, Ramsey-comb spectroscopy of the $1S - 2S$ transition in He$^+$ ions looks promising with a 1.9 ms excited state lifetime and the sufficiently strong pulses for high-harmonic generation [16].

[1] R. Holzwarth, T. Udem, T. W. Hänsch, J. C. Knight, W. J. Wadsworth, and P. S. J. Russell, Phys. Rev. Lett. **85,** 2264 (2000).

[2] D. J. Jones, S. A. Diddams, J. K. Ranka, A. Stentz, R. S. Windeler, J. L. Hall, and S. T. Cundiff, Science **288,** 635 (2000).

[3] A. Matveev, C. G. Parthey, K. Predehl, J. Alnis, A. Beyer, R. Holzwarth, T. Udem, T. Wilken, N. Kolachevsky, M. Abgrall, D. Rovera, C. Salomon, P. Laurent, G. Grosche, O. Terra, T. Legero, H. Schnatz, S. Weyers, B. Altschul, and T. W. Hänsch, Phys. Rev. Lett. **110,** 230801 (2013).

[4] C. G. Parthey, A. Matveev, J. Alnis, B. Bernhardt, A. Beyer, R. Holzwarth, A. Maistrou, R. Pohl, K. Predehl, T. Udem, T. Wilken, N. Kolachevsky, M. Abgrall, D. Rovera, C. Salomon, P. Laurent, and T. W. Hansch, Phys. Rev. Lett. **107,** 203001 (2011).

[5] M. Fischer, N. Kolachevsky, M. Zimmermann, R. Holzwarth, T. Udem, T. W. Hänsch, M. Abgrall, J. Grünert, I. Maksimovic, S. Bize, H. Marion, F. P. Dos Santos, P. Lemonde, G. Santarelli, P. Laurent, A. Clairon, C. Salomon, M. Haas, U. D. Jentschura, and C. H. Keitel, Phys. Rev. Lett. **92,** 230802 (2004).

[6] A. Antognini et al., Science **339,** 417 (2013).

[7] R. Pohl, R. Gilman, G. A. Miller, and K. Pachucki, Annu. Rev. Nucl. Part. Sci. **63,** 175 (2013).

[8] A. Beyer, J. Alnis, K. Khabarova, A. Mateev, C. G. Parthey, D. C. Yost, R. Pohl, T. Udem, T. W. Hänsch, and N. Kolachevsky, Ann. Phys. (Berlin) **525,** 671 (2013).

[9] S. Galtier, H. Fleurbaey, S. Thomas, L. Julien, F. Biraben, and F. Nez, J. Phys. Chem. Ref. Data **44,** 031201 (2015).

[10] D. C. Yost, A. Matveev, A. Grinin, E. Peters, L. Maisenbacher, A. Beyer, R. Pohl, N. Kolachevsky, K. Khabarova, T. W. Hänsch, and T. Udem, Phys. Rev. A **93,** 042509 (2016).

[11] A. Antognini et al., Eur. Phys. J. Web Conf. **113,** 01006 (2016).

[12] M. Herrmann, M. Haas, U. D. Jentschura, F. Kottmann, D. Leibfried, G. Saathoff, C. Gohle, A. Ozawa, V. Batteiger, S. Knünz, N. Kolachevsky, H. A. Schüssler, T. W. Hänsch, and T. Udem, Phys. Rev. A **79,** 052505 (2009).

[13] J. Komasa, K. Piszczatowski, G. Lach, M. Przybytek, B. Jeziorski, and K. Pachucki, J. Chem. Theory Comput. **7,** 3105 (2011).

[14] K. Pachucki and J. Komasa, J. Chem. Phys. **144,** 164306 (2016).

[15] W. Ubachs, J. C. J. Koelemeij, K. S. E. Eikema, and E. J. Salumbides, J. Mol. Spectrosc. **320,** 1 (2016).

[16] D. Z. Kandula, C. Gohle, T. J. Pinkert, W. Ubachs, and K. S. E. Eikema, Phys. Rev. Lett. **105,** 063001 (2010).

[17] A. Cingöz, D. C. Yost, T. K. Allison, A. Ruehl, M. E. Fermann, I. Hartl, and J. Ye, Nature (London) **482,** 68 (2012).

[18] C. Gohle, T. Udem, M. Herrmann, J. Rauschenberger, R. Holzwarth, H. A. Schuessler, F. Krausz, and T. W. Hänsch, Nature (London) **436,** 234 (2005).

[19] A. Ozawa, W. Schneider, T. W. Hänsch, T. Udem, and P. Hommelhoff, New J. Phys. **11,** 083029 (2009).

[20] J. Morgenweg, I. Barmes, and K. S. E. Eikema, Nat. Phys. **10,** 30 (2014).

[21] J. Morgenweg and K. S. E. Eikema, Phys. Rev. A **89,** 052510 (2014).

[22] N. F. Ramsey, Phys. Rev. **78,** 695 (1950).

[23] B. Gross, A. Huber, M. Niering, M. Weitz, and T. W. Hansch, Europhys. Lett. **44,** 186 (1998).

[24] S. Witte, R. T. Zinkstok, W. Ubachs, W. Hogervorst, and K. S. E. Eikema, Science **307,** 400 (2005).

[25] J. Morgenweg and K. S. E. Eikema, Opt. Lett. **37,** 208 (2012).

[26] J. Morgenweg and K. S. E. Eikema, Opt. Express **21,** 5275 (2013).

[27] A. Ozawa and Y. Kobayashi, Phys. Rev. A **86,** 022514 (2012).

[28] I. Barmes, S. Witte, and K. S. E. Eikema, Nat. Photonics **7,** 38 (2013).

[29] I. Barmes, S. Witte, and K. S. E. Eikema, Phys. Rev. Lett. **111,** 023007 (2013).

[30] S. Hannemann, E. J. Salumbides, and W. Ubachs, Opt. Lett. **32,** 1381 (2007).

[31] E. Gilabert, B. Lavielle, B. Thomas, S. Topin, F. Pointurier, and C. Moulin, J. Anal. At. Spectrom. **31,** 994 (2016).

[32] G. D. Dickenson, M. L. Niu, E. J. Salumbides, J. Komasa, K. S. E. Eikema, K. Pachucki, and W. Ubachs, Phys. Rev. Lett. **110,** 193601 (2013).